View metadata, citation and similar papers at core.ac.uk

brought to you by CORE

東北大学機関リポジトリ
TOUR
Tohoku University Repository

Experimental demonstration of thermoacoustic energy conversion in a resonator

著者	Biwa Tetsushi, Tashiro Yusuke, Mizutani Uichiro, Kozuka Motoki, Yazaki Taichi
journal or publication title	Physical Review. E
volume	69
number	6
page range	066304
year	2004
URL	http://hdl.handle.net/10097/52942

doi: 10.1103/PhysRevE.69.066304

Experimental demonstration of thermoacoustic energy conversion in a resonator

Tetsushi Biwa, Yusuke Tashiro, and Uichiro Mizutani
Department of Crystalline Materials Science, Nagoya University, Nagoya 464-8603, Japan

Motoki Kozuka
Department of Applied Physics, Nagoya University, Nagoya 464-8603, Japan

Taichi Yazaki
Aichi University of Education, Kariya, 448-8542, Japan

(Received 10 October 2003; published 10 June 2004)

Using thermoacoustic energy conversions, both amplification and damping of acoustic intensity are demonstrated. A differentially heated regenerator is installed near the velocity node of the resonator and thereby a high specific acoustic impedance and a traveling wave phase are obtained. It is shown that the gain of acoustic intensity resulting from the traveling wave energy conversion reaches 1.7 in a positive temperature gradient and 0.3 in a negative gradient. When the regenerator is replaced with a stack, it is found that the gain reaches 2.3, exceeding the temperature ratio (=1.9) of both ends of the stack. This is brought about by the addition of standing wave energy conversion. The present results would contribute to the development of new acoustic devices using thermoacoustic energy conversion.

DOI: 10.1103/PhysRevE.69.066304 PACS number(s): 47.90.+a, 43.25.+y, 43.35.+d, 43.38.+n

I. INTRODUCTION

The acoustic intensity I represents the time-averaged dynamic power flux sustained by oscillating motion of gas parcels in an acoustic wave. In ordinary speech, the acoustic intensity I is only on the order of 10^{-7} W/m^2 at most, but in a thermoacoustic heat engine, an I reaching 10^5 W/m^2 has been achieved using thermally induced spontaneous gas oscillations without the use of mechanical drivers [1]. Here the acoustic intensity I for a wave in a tube is written as

$$I = \langle PU \rangle = \tfrac{1}{2}\, pu \cos \Phi, \tag{1}$$

where the pressure $P = pe^{i\omega t}$, the cross sectional mean velocity of the oscillating gas $U = ue^{i(\omega t+\Phi)} = u \sin \Phi e^{i(\omega t+\pi/2)} + u \cos \Phi e^{i\omega t}$, angular brackets represent time average, and ω and Φ are an angular frequency and the phase lead of U relative to P, respectively. Production of higher acoustic intensity I is necessary to increase the potential utility of thermoacoustic engines in applications such as the liquefaction of natural gas [2].

Thermoacoustic energy conversion [3–5] between the axial heat flux Q [6] and I results from thermal interactions between gas parcels and solid walls of flow channels. As we will show in more detail in the next section, the traveling wave component (TWC) $u \cos \Phi$, in phase with P, performs Stirling cycles through the reversible heat exchange process between gas parcels and solid walls in the *regenerator* [1,7–11]. On the other hand, the standing wave component (SWC) $u \sin \Phi$ of U, out of phase with P by $\pi/2$, contributes to the energy conversion through irreversible heat exchange process with the *stack* of plates [5,12,13].

Ceperley [7] attempted to amplify I using thermoacoustic energy conversion based on the TWC. He installed a regenerator into a traveling wave field in a long tube having an acoustic driver at the end, and heated one end of the regenerator in a way such that the traveling wave passed through the regenerator from the cold end to the hot end. The energy conservation law assures the relation

$$\Delta(Q + I) = 0, \tag{2}$$

for Q and I in the regenerator, where Δ represents the difference in respective quantities between both ends of the regenerator. Therefore, when the output power $\Delta I > 0$ is produced through thermoacoustic energy conversions, the outgoing intensity I_{out} from the regenerator becomes larger than the incoming intensity I_{in} by the amount of ΔI. However, Ceperley only observed lower damping of I than that without heat flow Q, not the amplification of I. He attributed it to a large viscous loss caused by a low specific acoustic impedance $z = p/u = \rho_0 c$ inherent in a pure traveling wave, where ρ_0 and c represent mean density and sound speed, respectively.

In this paper, we demonstrate the occurrence of both thermoacoustic amplification and damping of I, depending on the direction of the temperature gradient imposed on the regenerator inserted in an acoustic resonator. We show that a high specific acoustic impedance reaching $15\rho_0 c$ and a traveling wave phase $\Phi = 0$ are achieved at a velocity node in the present resonator. By installing the regenerator at different positions near the velocity node, we varied the phase difference Φ between P and U in the regenerator to change the ratio of the TWC to the SWC responsible for the energy conversion. As a result of the dominant contribution due to the TWC in the regenerator, we obtained the gain $I_{\mathrm{out}}/I_{\mathrm{in}}$ of 1.7 when a positive temperature gradient was applied, and 0.3 with a negative one. When the stack was used instead of the regenerator, the gain of I reached 2.3, exceeding the temperature ratio at both ends of the stack. This is brought about by the addition of the SWC contribution to the traveling wave energy conversion.

 ©2004 The American Physical Society

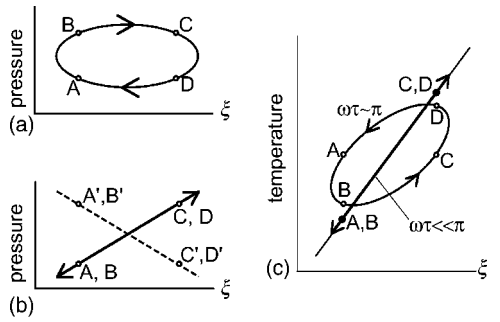

FIG. 1. The thermodynamic process for a gas parcel. The gas parcel experiences the TWC (a) and SWC (b) based displacements along with P, which are shown as an ellipse (a), solid ($\Phi>0$) and dashed ($\Phi<0$) lines (b) and on a P-ξ diagram, respectively. The temperature of a gas parcel (c) in the regenerator with good thermal contact is given by the tilted single line, but that with poor thermal contact traces an ellipse due to the relaxation time τ. The thin tilted line represents the wall temperature.

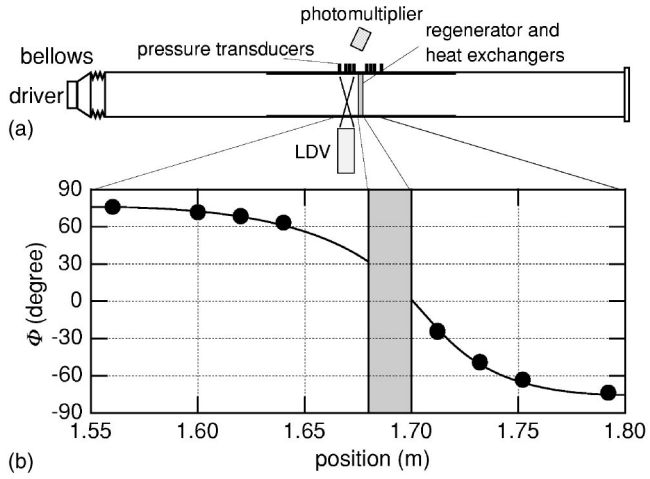

FIG. 2. Schematic illustration of the present experimental apparatus (a), the axial distributions of Φ (b) in the middle of the resonator. The assembly of a regenerator and two heat exchangers are represented by a gray region.

II. THERMOACOUSTIC ENERGY CONVERSION

We briefly describe here the thermoacoustic energy conversion executed by the gas parcels. The displacement ξ of a gas parcel from its equilibrium position is simply written from the expression of U as

$$\xi = \frac{u}{\omega}\cos\Phi e^{i(\omega t-\pi/2)} + \frac{u}{\omega}\sin\Phi e^{i\omega t}. \tag{3}$$

We denote the first and the second terms on the right-hand side of Eq. (3) as TWC-based and SWC-based displacement, respectively. They trace a clockwise ellipse and a straight line with a finite slope on a P-ξ plane during one cycle of the acoustic wave, as shown in Figs. 1(a) and 1(b). A gas parcel on the P-ξ plane experiences cyclic compression and expansion processes while exchanging heat with the walls in the flow channel.

The nature of the heat exchange process is well represented in terms of a nondimensional parameter $\omega\tau$ [4], where τ represents the thermal relaxation time given by using the characteristic transverse length r_0 and the thermal diffusivity α of the gas as $r_0^2/(2\alpha)$ [14]. If $\omega\tau \ll \pi$, the gas in the channel moves reversibly in equilibrium with the local temperature at the wall in contact with it, whereas if $\omega\tau \gg \pi$, the gas motion becomes isentropic but still reversible. The gas oscillation becomes thermodynamically irreversible near $\omega\tau \approx \pi$ due to incomplete heat transfer to the wall. A porous medium having flow channels with $\omega\tau < \pi$ is usually called a "regenerator." On the other hand, a porous medium with $\omega\tau \approx \pi$ is called a "stack."

Figure 1(c) presents the axial distribution of the wall temperature (thin line). Also shown is the variation of the absolute temperature T of the gas parcels due to the displacement ξ in the temperature gradient. When $\omega\tau \ll \pi$, T always traces the local wall temperature, because the gas parcel is instantaneously heated and cooled because of its good thermal contact with the wall. On the other hand, the gas parcel does not exchange heat with the walls when $\omega\tau \gg \pi$. Near $\omega\tau \approx \pi$, the finite relaxation time τ causes a time delay in heating and cooling over the cross section of the flow channel, thus the T-ξ diagram traces an ellipse.

The thermodynamic cycle executed in the course of the TWC-based displacement is given by combining Figs. 1(a) and 1(c). Starting from the position near the left end labeled "A" in Fig. 1(a), the gas parcel repeats a cyclic motion consisting of compression (A-B)–heating(B-C)–expansion (C-D)–cooling(D-A), when $\omega\tau \ll \pi$. As Ceperley has noted [7], this is a thermodynamic cycle similar to the Stirling one, thereby enabling an amplification of the acoustic intensity I. The TWC also contributes to the energy conversion even when $\omega\tau \approx \pi$, but poor thermal contact with the wall leads to heat losses.

During the SWC-based displacement shown in Fig. 1(b), the gas parcel experiences heating and compression at the same time when it moves to the hot end (B-C), while it simultaneously experiences cooling and expansion when it moves back to the cold end (D-A). Therefore, the SWC does not contribute to the energy conversion when $\omega\tau \ll \pi$. However, as is discussed by Wheatley [5], a finite τ in the heat exchange process causes a phase lag in the heating and cooling of the gas parcel. This establishes a thermodynamic cycle of compression (B-C)–heating(C-D)–expansion (D-A)–cooling(A-B). Thus, the SWC energy conversion takes place when $\omega\tau \approx \pi$.

III. EXPERIMENT

A. Experimental apparatus

The present experimental apparatus is schematically illustrated in Fig. 2(a). A middle section of the cylindrical acoustic resonator is constructed of Pyrex glass tube with a 21 mm inner diameter to allow the measurement of the velocity of the gas by means of a laser Doppler velocimeter (LDV). The remaining part of the resonator is constructed of stainless steel tubing. The total length of the resonator is 3.3 m. One

end of the resonator is closed by a woofer speaker through dynamic bellows, and the other is closed by a solid plate. The speaker is driven at 103 Hz. Air at local atmospheric pressure is used as the working gas. Either a regenerator or a stack, each being 20 mm long, is inserted near the middle of the resonator.

Hot and cold heat exchangers, consisting of brass strips aligned in parallel, are placed at both sides of a regenerator and a stack in order to produce temperature gradients along them. The hot heat exchanger is heated by a resistance heater up to $T_H=560$ K, and the cold heat exchanger is kept at room temperature ($T_C=296$ K) using running water. Positive and negative temperature gradients are formed by changing the location of the two heat exchangers with each other.

We use a pile of stainless screen meshes (60 mesh) with $r_0=0.15$ mm as the regenerator and a ceramic catalyst with $r_0=0.77$ mm as the stack. The values of $\omega\tau$ are estimated as 0.13 for the regenerator and 3.5 for the stack, respectively, where α at the mean temperature $[=(T_H+T_C)/2]$ is used for the evaluation. As we will see later, the TWC contributes almost exclusively to the energy conversion in the present regenerator, while the SWC has the major contribution in the stack.

B. Pressure and velocity measurements

The pressure $P=pe^{i\omega t}$ along the glass tube was measured using small pressure transducers (Toyoda Koki, DD102-1F), which were mounted on the tube wall via short ducts of 10 mm in length and 1 mm in inner radius. We measured the axial core velocity at the center of the cylinder with an LDV, and determined both amplitude u and phase Φ in the cross sectional mean velocity $U=ue^{i(\omega t+\Phi)}$ from the measured values by applying laminar flow theory. Pressure and velocity signals were collected by a 24-bit spectrum analyzer. Using power and phase spectra, we determined p, u, and Φ. It was important to determine precisely the instrumental time delay of the LDV ($=2.7\times10^{-5}$ s) for the accurate evaluation of Φ and hence I [13,15].

C. Acoustic field in a resonator

Before showing the experimental data on the acoustic intensity I, we present the acoustic field excited in the resonator and its advantages for this experiment. In this experiment, we used the second resonance mode having a velocity node at the middle of the resonator. We found that this mode occurs at 103 Hz with a quality factor Q_r of 30 from the measurement of frequency response curves.

Figure 2(b) shows the axial distribution of Φ in the vicinity of the room temperature regenerator at a position 1.69 m away from the speaker. If a nondissipative standing wave were formed in the resonator with a very high Q_r, Φ would take 90° or −90°, depending on whether the sign of the gradient of p is positive or negative. However, in the present resonator with the finite $Q_r\approx30$, it was found that Φ continuously varied in the range $-90°<\Phi<90°$ and passed zero at the velocity node. This continuous variation shows that the ratio of TWC to SWC varies as a function of the axial position along the resonator. In Fig. 2(b), we see that the phase Φ_m in the center of the regenerator is 20°. Thus, we can choose a desired ratio of TWC to SWC in the center of the regenerator by shifting its axial position. This is the clear advantage of the use of the resonator in this experiment.

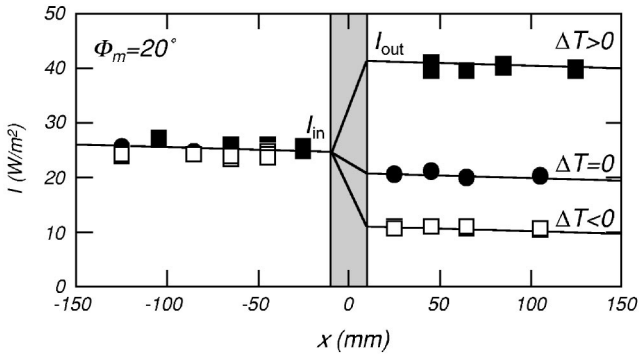

FIG. 3. Axial distribution of I obtained for different temperature gradients measured when $\Phi_m=20°$. A gray area represents the assembly of a regenerator and two heat exchangers.

We have found that the specific acoustic impedance z given as p/u reaches $15\rho_0c$ near the velocity node in the present resonator. Hence, the gas parcel at the velocity node oscillates with both a high acoustic impedance z and a traveling wave phase $\Phi=0$. This is another advantage of the use of the acoustic field in the resonator [11] over the pure traveling wave propagating through a long tube, in which z is given by ρ_0c [7]. Thus, we can demonstrate the thermoacoustic energy conversions without suffering from strong viscous damping by installing the regenerator close to the velocity node.

IV. RESULTS AND DISCUSSION

A. Axial distribution of acoustic intensity

We report here the axial distribution of acoustic intensity I, when Φ_m is 20° and the temperature gradient is zero along the regenerator as shown in Fig. 2(b). We inserted the measured p, u, and Φ into Eq. (1), and plotted I thus obtained in Fig. 3. The origin of x is taken at the center of the regenerator. The error in I, mostly due to the uncertainty in Φ, is within the size of the markers. The positive value of I indicates that I flows through the resonator from the acoustic driver to the closed end. The negative slope of I represents the dissipative energy per unit volume due to the viscosity and the thermal conductivity of the working gas. The value of the slope is found to be approximately -12 W/m^3 in the region outside the regenerator and -120 W/m^3 inside of it.

We supplied heat power to the regenerator to create temperature gradients on it. Here we kept $\Phi_m=20°$ and also adjusted the incoming acoustic intensity I_{in} to the regenerator to be the same as that without the heat power. When a positive temperature gradient $\nabla T>0$ is formed along the regenerator, I propagates through the regenerator from the cold to the hot end. We clearly see the formation of a steep positive slope in I in the regenerator. This demonstrates the thermoacoustic amplification of I, which Ceperley had attempted to

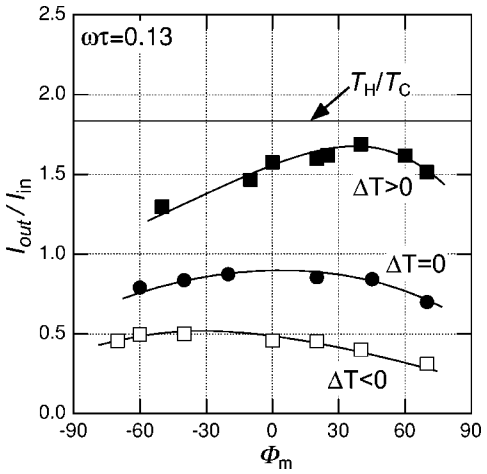

FIG. 4. The amplification rate I_{in}/I_{out} as a function of Φ_m determined for the regenerator. Three different symbols represent the data with positive (solid squares), negative (open squares) temperature gradients and without a temperature gradient (solid circles). A horizontal line represents the temperature ratio T_H/T_C. The error of the data does not exceed the size of the markers.

observe [7]. The gain defined as I_{out}/I_{in} turned out to be 1.6. This is caused by the positive output power $I_{out}-I_{in}$ resulting from the thermoacoustic energy conversions.

On the other hand, I flows from hot to cold through the regenerator when a negative ∇T is set up. Apparently, I decreases more significantly for this case in the regenerator region than that with $\nabla T=0$. The gain I_{out}/I_{in} was found to be 0.45. This result shows the strong thermoacoustic damping of I executed by the gas parcels when $\Phi_m=20°$. While conventional silencers rely on viscous and thermal attenuation of the acoustic wave as shown in the data with $\nabla T=0$, a thermoacoustic silencer uses energy conversions between I and Q in addition to them to achieve a strong damping. Now we are ready to study how the gain I_{out}/I_{in} changes as a function of Φ_m by shifting the position of the regenerator in the resonator.

B. Regenerator ($\omega\tau=0.13$)

Figure 4 shows the gain I_{out}/I_{in} as a function of Φ_m, when the regenerator with $\omega\tau=0.13$ is employed. The value of $\omega\tau=0.13$ assures good thermal contact between gas parcels and screen meshes in the regenerator, thereby allowing us to neglect the contribution of the SWC to the energy conversion in this regenerator. When ∇T is absent, I_{out}/I_{in} consistently lies below unity, which shows that I decreases in the regenerator. It is also found that the gain I_{out}/I_{in} shows a maximum centered at $\Phi_m=0°$. This represents that the energy loss in the regenerator is minimized when the center of the regenerator is placed at the velocity node, but it becomes large when the regenerator is placed away from the velocity node. Thus, the viscous loss dominates in the present regenerator.

When a positive ∇T is created along the regenerator, I_{out}/I_{in} is increased well beyond unity, demonstrating the amplification of I in the regenerator. Also we see that I_{out}/I_{in} with $\nabla T>0$ shows a maximum reaching 1.7 at $\Phi_m\approx 40°$. This corresponds to the situation where the hot end of the regenerator is placed at the velocity node. Stirling prime movers based on the TWC energy conversion under perfect thermal contact in the regenerator should attain a gain I_{out}/I_{in} equal to the temperature ratio T_H/T_C when an inviscid ideal gas is used as the working fluid [7]. The fact that the highest I_{out}/I_{in} we obtained is still less than the ratio T_H/T_C of 1.9 would be attributed to the unavoidable viscous loss in the regenerator, as we have seen in the data with $\nabla T=0$. However, since the kinematic viscosity ν of the gas increases with increasing temperature, viscous losses should become relatively larger at the hot end than that at the cold end, even if the velocity amplitude is the same at both ends of the regenerator. Thus, the Φ_m yielding minimum viscous losses should be positive so that the velocity node comes close to the hot end. Therefore, we consider that the gain shows a maximum at $\Phi_m\approx 40°$ instead of $\Phi_m=0$. If the specific acoustic impedance z becomes much higher than in the present experiment, the maximum I_{out}/I_{in} would essentially approach T_H/T_C.

When a negative ∇T is present, the decrease of I along the regenerator becomes significantly larger than that with $\nabla T=0$. As a result, the gain I_{out}/I_{in} lies far below that with $\nabla T=0$ and becomes 0.3 with $\Phi_m=70°$, as shown in Fig. 4. When a negative ∇T is present along the regenerator, the gas parcels experience cooling when it moves from B to C in Fig. 1(a), and heating when it moves from D to A. As a result, the thermodynamic cycle of compression (A-B)−cooling(B-C)−expansion(C-D)−heating(D-A) is executed in the course of the TWC-based displacement. This is the reversed Stirling cycle that makes ΔI negative. Therefore, the thermoacoustic energy conversion is responsible for the strong damping of I. We see that the gain I_{out}/I_{in} shows a peak at $\Phi_m\approx -40°$. This means that minimum damping is obtained when the velocity node comes to the hot end of the regenerator for the same reason as that described above when ∇T is positive.

C. Stack ($\omega\tau=3.5$)

Next, we used a stack of $\omega\tau=3.5$ instead of the regenerator. Results are shown in Fig. 5. When ∇T is zero, I_{out}/I_{in} for the stack lies below unity as in the regenerator, but shows a broader peak than that for the regenerator. While viscous losses dominated in the regenerator, the dissipation due to the thermal conduction over the cross section of flow channels, which is proportional to p^2 [4], becomes large in the present stack. The stack is always located around the pressure antinode (velocity node) in this experiment, and hence the value of p in the stack is not affected much by the value of Φ_m. Thus, we see that the thermal conduction causes the broad peak centered around $\Phi_m=0°$.

When a positive ∇T is set up along the stack, the gain I_{out}/I_{in} for the stack is clearly different from that for the regenerator; it monotonically increases with increasing Φ_m. Eventually, I_{out}/I_{in} reached 2.3 at $\Phi_m=80°$, which is larger than $T_H/T_C=1.9$, when the center of the stack is placed 10 cm away from the velocity node toward the acoustic driver. The contribution of the TWC to the energy conversion can be seen at $\Phi_m=0°$, since the SWC is absent there.

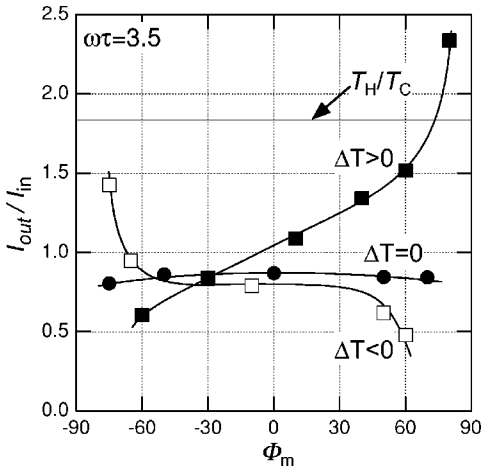

FIG. 5. The amplification rate I_{in}/I_{out} as a function of Φ_m determined for the stack. Three different symbols represent the data with positive (solid squares), negative (open squares) temperature gradients and without a temperature gradient (solid circles). A horizontal line represents the temperature ratio T_H/T_C. The error of the data does not exceed the size of the markers.

We see that I_{out}/I_{in} is nearly equal to unity. This represents that the amplification due to the TWC is so small that it is used up to compensate for the dissipative energy in the stack. Therefore, the observed large enhancement of I_{out}/I_{in} should reflect the thermoacoustic energy conversion due to the SWC. Indeed, as we described in Sec. II, the SWC with a positive Φ_m contributes to the amplification of I in the presence of a positive ∇T. Thus,the present results clearly demonstrate that amplification of I exceeding T_H/T_C, the gain expected for an ideal regenerator, is made possible by using the SWC energy conversion in the stack.

In a standing wave thermoacoustic prime mover, the acoustic intensity I comes out of both sides of the stack [13] placed between the velocity node and antinode. When a ∇T is positive in the stack, the acoustic intensity I at the cold end is negative, while that at the hot end is positive. Therefore, I_{in} in the standing wave prime mover is zero, because I is generated within the stack. This represents that the gain I_{out}/I_{in} can be very large when the SWC mostly contributes to the energy conversion. Therefore, as the present results indicate, the use of the SWC energy conversion is of great importance when one attempts to make the gain I_{out}/I_{in} as high as possible in a given temperature ratio.

When the stack is placed beyond the velocity node, Φ_m becomes negative and the gain I_{out}/I_{in} decreases below unity in spite of a positive ∇T. This is because the sign of the slope in the P-ξ diagram is reversed when Φ_m is negative. As shown by the dashed line in Fig. 1(b), the gas parcels with negative Φ_m experience expansion when they move from left(B') to right(C'). Hence, the gas parcel undergoes the thermodynamic process in the order of expansion(B'-C')−heating(C'-D')−compression(D'-A')−cooling(A'-B'), which leads to the reversed cycle discussed in Sec. II. As a result, the SWC contributes to the reduction of I when Φ_m is negative in the presence of a positive ∇T.

When a negative ∇T is made along the stack, the gain I_{out}/I_{in} increases with decreasing Φ_m and it exceeds unity when $\Phi_m < -60°$. Since the TWC with a negative ∇T always contributes to the damping of I regardless of the sign of Φ_m, the amplification of I must be due to the SWC. As is described above, a negative Φ_m reverses the order of compression and expansion in the cycle. On the other hand, in the presence of a negative ∇T, the order of heating and cooling is also reversed. Consequently, gas parcels experience the cycle yielding a positive ΔI during the SWC-based displacement, when both Φ_m and ∇T are negative. On the other hand, with a positive Φ_m, both the SWC and TWC contribute to the damping of I. Thus, the gain I_H/I_C lies far below unity with a positive ∇T.

It is clear from the argument above that Φ_m must be positive in order to obtain a gain as large as possible in a thermoacoustic power amplifier, because both the TWC and SWC can contribute to the amplification of I, when $\nabla T > 0$. The maximum I_{out}/I_{in}, exceeding T_H/T_C at $\Phi_m = 80^\circ$ obtained in this experiment, apparently results from the energy conversion both due to the TWC and SWC. However, while the efficiency of the energy conversion due to the TWC can ideally reach Carnot's efficiency, that due to the SWC is essentially lower than that due to the TWC, since the SWC energy conversion intrinsically relies on the irreversible heat exchange process [3–5,7]. Thus, in order to achieve both high efficiency and gain under a given temperature ratio, one has to choose an optimum Φ_m to give the best combination of the TWC and SWC. As shown in Figs. 4 and 5, the optimum Φ_m should depend on the value of $\omega\tau$ of a given regenerator. By using a series of regenerators and stacks inserted at positions with proper Φ_m, we could obtain very high acoustic intensity I such as those used in practical engines.

V. SUMMARY

We demonstrated thermoacoustic energy conversions by making full use of the acoustic field induced in the resonator. Through the simultaneous measurements of P and U, we determined the gain of the acoustic intensity I and the phase angle Φ between P and U. We found that the regenerator worked as a thermoacoustic power amplifier with a gain of 1.7 when ∇T was positive, but as a silencer with a gain of 0.3 when ∇T was negative. These results obtained for the regenerator originates from the energy conversion due to the TWC. Furthermore, the SWC was found to play the major role in the energy conversion in the stack. Especially when $\Phi_m = 80^\circ$ and $\nabla T > 0$, the gain I_{out}/I_{in} reached 2.3 resulting from the SWC energy conversion. This represents that the addition of the SWC to the TWC makes it possible to increase the gain above the temperature ratio T_H/T_C, the ideal gain for the Stirling engine. By placing the regenerators and stacks near the velocity nodes in a long acoustic resonator and amplifying I successively, we would be able to obtain a very high acoustic intensity I even from waste heat having a low energy density. The present results will contribute to the development of new acoustic devices using thermoacoustic power amplifiers and silencers.

[1] S. Backhaus and G. W. Swift, Nature (London) **399**, 335 (1999).
[2] J. J. Wollan, G. W. Swift, S. N. Backhaus, and D. L. Gardner (unpublished).
[3] G. W. Swift, *Thermoacoustics: A Unifying Perspective for Some Engines and Refrigerators* (Acoustical Society of America, Publications, Sewickley, PA, 2002).
[4] A. Tominaga, Cryogenics **35**, 427 (1995); *Fundamental Thermoacoustics* (Uchida Roukakuho Publishing, Tokyo, 1998).
[5] J. Wheatley, T. Hofler, G. W. Swift, and A. Migliori, Phys. Rev. Lett. **50**, 499 (1983); J. Acoust. Soc. Am. **74**, 153 (1983); Am. J. Phys. **53**, 147 (1985).
[6] Heat flux due to the oscillating gas is defined as $Q=T_m S$ using the mean temperature T_m and entropy flow S. The entropy flow S is given as $S=\rho_m\overline{\langle s\cdot U\rangle}$, where angular brackets and a bar represent time and radial averages, ρ_m, s, and U are, respectively, the mean mass density, entropy per unit mass, and axial velocity for the oscillating gas.
[7] P. H. Ceperley, J. Acoust. Soc. Am. **66**, 1508 (1979).
[8] T. Yazaki, A. Iwata, T. Maekawa, and A. Tominaga, Phys. Rev. Lett. **81**, 3128 (1998).
[9] T. Yazaki, T. Biwa, and A. Tominaga, Appl. Phys. Lett. **80**, 157 (2002).
[10] Y. Ueda, T. Biwa, U. Mizutani, and T. Yazaki, Appl. Phys. Lett. **81**, 5252 (2002); J. Acoust. Soc. Am. **115**, 1134 (2004).
[11] G. Petculescu and L. A. Wilen, ARLO **3**, 71 (2002).
[12] A. A. Atchley, J. Acoust. Soc. Am. **95**, 1661 (1994).
[13] T. Yazaki and A. Tominaga, Proc. R. Soc. London, Ser. A **454**, 2113 (1998).
[14] A nondimensional parameter $\omega\tau$ is related to the thermal penetration depth $\delta=\sqrt{2\alpha/\omega}$ as $\omega\tau=(r_0/\delta)^2$.
[15] T. Biwa, Y. Ueda, T. Yazaki, and U. Mizutani, Cryogenics **41**, 305 (2001).